Desalination and Water Treatment
www.deswater.com

doi: 10.1080/19443994.2015.1123191

57 (2016) 11639–11659
May

Taylor & Francis
Taylor & Francis Group

Hydrological and rating curve modelling of Pinios River water flows in Central Greece, for environmental and agricultural water resources management

Evangelos Hatzigiannakis, Agathos Filintas*, Andreas Ilias, Andreas Panagopoulos, George Arampatzis, Ioannis Hatzispiroglou

Soil and Water Resources Institute – Land Reclamation Department, Hellenic Agricultural Organisation-DG Research (N.AG.RE.F.), 57400 Sindos-Thessaloniki, Greece, Tel. +30 2310798790; emails: hatzigiannakis@gmail.com (E. Hatzigiannakis), ag.filintas@gmail.com (A. Filintas), anilias.LRI@nagref.gr (A. Ilias), panagopoulosa@gmail.com (A. Panagopoulos), arampgeo@gmail.com (G. Arampatzis), chatzispyroglou@gmail.com (I. Hatzispiroglou)

Received 6 February 2015; Accepted 15 November 2015

ABSTRACT

The aim of the present study is a hydrological approach on streamflow modelling, in order to investigate flow velocity, discharge rate, stage, river bed variations and the hydraulic properties (water depth, flow area, wetted perimeter, hydraulic radius and depth, Manning's coefficient of roughness, Froude Number, etc.) of the Pinios River at P145 Giannouli-Larissa monitoring station (Central Greece). Also, the study aims to the compilation–validation of a rating curve (RC) from a series of stage $h(t)$–discharge $Q(t)$ pairs measurements, in order to use them as tools to assist environmental and agricultural water resources management, support environmental flows estimation, monitoring and irrigation planning in local basin scale. The results and statistical analysis, showed that Froude number during the measurement period oscillated from a minimum 0.109 to maximum 0.283 (mean Fr = 0.172). Therefore, in all cases, Fr < 1 which means that streamflow of the River Pinios, at P145 station is classified as subcritical. The segment's maximum water velocity measured from a minimum 0.452 to maximum 1.693 m s^{-1} (mean 1.247). The mean monthly river discharges of years 1978, 1979 and 2014 were found to be 35.91, 57.52 and 50.37 m^3 s^{-1}, respectively. The summer months (June–August) of recent and also of historic years presented low to zero discharges, which are below the environmental flow lower (critical) limit. Moreover, based on the parameters' measurements from 2013 (July) up to 2014 (December), on the modelling analysis, on classification results and on the proposed model performance index (MPI) for each of the eight models tested, the power model was selected as the best to use for the compilation and best fit of the flow RC for this monitoring station. The results of model's validation using two different statistical methods, model simulation, error statistics criteria and the proposed MPI index, were converge to the same output that the data fitting the selected power model for the curve $RC_{(2013–2014)}$ was very satisfactory,

*Corresponding author.

Presented at the 12th International Conference on Protection and Restoration of the Environment (PRE XII) 29 June–3 July 2014, Skiathos Island, Greece

and the stability of the developed relationship was robust. The resulted streamflow RC and the extrapolated parts, the rainfall vs. discharge and environmental flows analysis, the river bed variation analysis and the performed hydraulic properties estimates are proposed to serve as hydrological assisting tools for environmental water resources and irrigation management at the study area. These assisting tools will help water authorities accurately and quickly estimate river's water quantities and variation with a minimum cost and effort, and they could be used for irrigation management, environmental flow estimation, groundwater recharge, flood protection and other purposes.

Keywords: Rating curve modelling; Streamflow measurements; Water resources engineering; Water velocity and discharge; Froude number; Hydraulic properties; Model validation; Simulation and error estimation

1. Introduction

River flow velocity, discharge, stage, hydraulic depth and type of flow are major topics in engineering hydrology and they are directly related to water supply, quality and management, flood control, drainage, irrigation, reservoir design and other relative issues.

Flow velocity in rivers has a major impact on the residence time of water and thus on high and low water level as well as on water quality [1]. So, river flow velocity is the variable usually required for hydrological analysis of a river hydrosystem. Unfortunately, the continuous measurement of the stream flow that passes through a river cross-section is usually impractical or prohibitively expensive [2–8]. However, when a rating curve (RC) is constructed based on a series of stage $h(t)$ and discharge $Q(t)$ pairs measurements, a river's cross-section can be observed continuously or at regular short-time intervals (weekly, monthly, etc.) only for stage with relative ease and economy [9,10]. Streamflow, or discharge, is defined as the volume rate of flow of the water including any sediment or other solids that may be dissolved or mixed with it, that passes through a given river/stream section at a given time [4,6]. Fortunately, a relation may be deduced between stage and the corresponding discharge at a given river cross-section. This relation is termed a stage–discharge relationship or stage–discharge RC or simply, RC. The stage–discharge relationship is the relationship at a gauging station between stage and discharge and is sometimes referred to as a RC or rating [11–14]. This RC is established by making a number of concurrent observations of a river's stage $h(t)$ and discharge $Q(t)$, over a period of time covering the expected range of stages at the river measuring section.

A fast and accurate estimation of the river discharge is of great interest for a large number of environmental and engineering applications such as real-time flood forecasting and water resources management. Therefore, the knowledge of the $h - Q$ RC at a river section is important for this purpose [14]. River flow velocity is crucial to simulate discharge hydrographs [1–4,7–9,12] and the residence time of water in the hydrological system [1,8]. Records of streamflow are the basic data used in developing reliable surface water supplies because the records provide information on the availability of streamflow and its variability in time and space. The records are therefore used in the planning and design of surface water-related projects (agricultural and environmental management, irrigation, environmental flows estimation and monitoring), and they are also used in the management or operation of such projects after the projects have been completed.

Streamflow records are also used for calibrating hydrological models in catchments, which are used for forecasting, such as flow forecasting [15]. If a single or a limited number of catchments are modelled, complex flow velocity equations can be parameterized with observed catchment-specific values. This is not possible at larger scales [1]. A current meter measurement is the summation of the products of the partial areas of the stream cross-section and their respective average velocities. In the mid-section method by making current meter measurements at river locations, it is assumed that the velocity sample at each location represents the mean velocity in a partial rectangular area called segment [2–5,7–10,12–14]. The area extends laterally from half the distance from the preceding measurement location to half the distance till the next location and vertically, from the water surface to the corresponding depths of the river bed [4]. Using the $h(t) - Q(t)$ pairs' measurements and other hydraulic variable measurements of a river cross-section in conjunction with hydraulic modelling equations, we can calculate many hydraulic properties which are important tools in hydrological analysis and in RC mathematical compilation.

2. Materials and methods

2.1. Sample and data collection, instruments used and specifications

For the river flow velocity measurements a propeller flow velocity meter was used (Valeport Model 001) which is a current flow meter [16], operated with a suspension set, along with a digital measuring device including an electronic flow calculator, data logger and real-time control display unit. Data input of the digital measuring device may be averaged over any number of seconds from 1 to 600, or according to number of impeller revolutions. In the present study, the river flow data were averaged over a pair measurement of 60 + 60 s. Current flow measurements were conducted via suspension of the system over a bridge. An extended tail fin was used to ensure alignment of the instrument to the streamflow current. Suspension deployments were augmented by two different streamlined weights. The instrument used in the present study was calibrated by the manufacturer according to BS ISO 2537:2007 standards [17]. In the hydrometric practice of the present study, the stage h (t) measurements (in m) of the Pinios River with a specified by the authors' datum were performed over a high bridge at Giannouli Larissa monitoring station (station code P145) of the Pinios basin in Central Greece, manually with a hand suspension wire gauge–weight system, for measuring the distance to the water surface. The gauge datum was checked by levelling from local benchmarks. It is important to maintain the same gauge datum throughout the period of record. To avoid negative readings, the gauge and datum were set so that a reading of zero is below the lowest anticipated stage. Monitoring frequency for a particular station is selected on the basis of the rapidity with which the stage can change and its significance to change in discharge. Flashy streams require more frequent measurements and large streams allow for less frequent measurements [5,7–10,12]. In the present study, the time interval of flow and stage measurements occurred one to three times every month. Vertical observations of depth and velocity were performed in order to best define the variation in elevation of the river bed and the cross-section's variation in water velocity. In cases, where the weight on the sounding line was not sufficient to keep the line perpendicular to the water surface, a heavier weight was used in order to maintain the wire line perpendicular.

2.2. Methods and calculations

Measured river water flow velocity, depths and widths of the identified segments were used for the estimation of cross-section's mean flow velocity in each measured segment [4,5,7–11,13,18]. Following, the mid-section method was used for the overall discharge calculation of the river section, i.e. deploying all segments flow area [4,5,8]. The cross-section characteristics, the river flow velocity of each segment and the mean water flow velocity total profile at the discussed monitoring station (P145) were measured, calculated and annotated, respectively. A series of concurrent stage and flow measurements were performed from summer 2013 (July) to winter 2014 (December). Also, other observable (depth, segment width, river width, water flow velocity, stage) or estimated hydraulic variables (water mean depth, flow area, discharge, wetted perimeter, hydraulic depth, hydraulic radius, Manning's coefficient of roughness, Froude Number, etc.), were measured, estimated and annotated. The mathematical formula in Eq. (1) was used for the river flow velocity calculations:

$$V = a + \left(b_{\text{eq}} \cdot N_{\text{eq}}\right) \tag{1}$$

where V = flow velocity (m s^{-1}); a = starting velocity to overcome mechanical friction, b_{eq} = equipment calibration constant and N_{eq} = revolutions per second.

Measured water flow velocity (V (m s^{-1})) was then used for the computation of discharge, using the mid-section method. Discharge in each segment is computed by multiplying the average cross-section area of a segment by the mean flow velocity of that segment. The total discharge is the sum of these discharges [2–10,18,19]. Analytically, in the mid-section method, discharge Q (m^3 s^{-1}) in each segment is computed by multiplying $V \times d$ (V = mean flow velocity (m s^{-1}), d = mean depth (m)) in each vertical by a width distance b (m) of the segment, which is the sum of half the distances to adjacent verticals. The value of d in the two half widths next to the banks can be estimated using water depth measurements. Total discharge $Q(t)$ for each measurement date was computed using Eq. (2):

$$Q = V_1 d_1 \left(\frac{b_2 + b_1}{2}\right) + V_2 d_2 \left(\frac{b_3 + b_2}{2}\right) + \cdots + V_n d_n \left(\frac{b_n + b_{n-1}}{2}\right) \tag{2}$$

Then, stage $h(t)$ and discharge $Q(t)$ pairs were used in the study in order to establish a mathematical relationship between the discharge and the water level (stage) variable. The river's streamflow RC ($h - Q$) [1–5,7–11,18,20] and the river bed variation of the Pinios River at Giannouli station in Larissa, Central

Table 1
Classes and relative SC score weights used for scoring each error statistics criterion rank class k for the calculation of the Models' Performance Index (MPI)

Class k	1	2	3	4	5	6	7	8	Total
SC	20.00	18.00	16.00	13.50	11.00	9.00	7.00	5.50	100.00

Greece were calculated based on the measured data using various model equations (linear, logarithmic, inverse, compound, power, growth, exponential and logistic type) for regression, F test of model fit and ANOVA analysis with the aid of the statistical parcel SPSS software application (SPSS ver. 17), [21]. The discharge $Q(t)$ can then be routinely estimated by the stage $h(t)$ measurement via the RC.

2.3. Performance criteria and model performance index

The overall performance of the various data-driven models was evaluated by means of the following errors statistics criteria: (1) root mean squared error (RMSE), (2) coefficient of determination (R^2), (3) standard error of estimate (SEE), (4) mean absolute error (MAE) and (5) mean absolute discharge measurement per cent difference [MAD D(%)].

The evaluation of each errors statistics criterion is governed by the following evaluation rules:

(1) For the RMSE criterion, a better fit between observed and modelled data is obtained as its value approaches zero.
(2) For the coefficient of determination criterion, the closer R^2 is to ±1, the better the fit is.
(3) For the SEE criterion, the better fit between observed and modelled data is obtained as its value approaches zero.
(4) For the MAE criterion, the better fit between observed and modelled data is obtained as its value approaches zero.
(5) For the MAD D(%) criterion, the better fit between observed and modelled data is obtained as its value approaches zero.

Based on the results of aforementioned criteria, an approach of total weighted classification score of these criteria was used for the proposed model performance index (MPI) of the tested models in descending order from best to worst. The weights used for scoring each error statistics criterion rank class is given in Table 1.

The proposed MPI of each model was calculated using the mathematical Eq. (3). As the value of the MPI index approaches one, the better performance of the relative model is obtained:

$$\text{Index MPI} = \frac{\sum_{j=1}^{n} \left|\text{SCesc}_{(j,k)}\right|}{100}, \quad j = 1\ldots5, \quad k = 1\ldots8 \quad (3)$$

where esc = is the error statistics criterion and esc ∈ {RMSE, R^2, SEE, MAE, MAD D(%)}, j = is the number of models' error statistics criteria, SC = is the corresponded weighted classification score of the criterion j depending on assigned Class k.

Based on the statistical resulted value of each error statistics criterion (RMSE, R^2, SEE, MAE, MAD D(%)) for each model, a classification was performed between models criteria (esc) in order to rank the value of each criterion from best to worst in descending order, assigning it in a Class k according to the evaluation rules presented above. Then, depending on the results of the classification Class k for each criterion, the corresponded weighted classification score (SC) of the criterion is taken from Table 1. Finally, the scores (SC) of error statistics criteria are used along with the Eq. (3) in order to calculate the MPI (see an example of the power model MPI calculation below in section Results and Discussion). The relative SC score weights used for scoring each error statistics criterion rank Class k in Table 1, were taken as mean values after their grading by the scientific (experts) team.

2.4. Rainfall vs. discharge analysis, environmental flows and irrigation management

The rainfall data of the study area were processed (2013–2014 and 1978–1979), and analysed conjunctively with performed discharge measurements $Q(t)$ and historical discharge data, in the aspect of river flows, environmental flows and agricultural (irrigation) management.

2.5. Extrapolation modelling of the RC

A logarithmic extrapolation was performed based on the final RC ($RC_{(2013–2014)}$). In the upper part of the curve, extrapolation consisted of two subparts, where the first one was 1.5 times according to ISO 1100-2:1998 [12,14] and the second one was two times the highest measured discharge for the time period 2013–2014.

2.6. Model's validation

Model's validation, comparison and error estimation [22–25] were consisted from two separate parts. In the first part of model's validation, the cross-validation method was fully applied on data, based on the recent sample data set with the $h(t)$ and $Q(t)$ measurements for years 2013–2014. In the second part, the validation method between two sample data sets was fully applied on the recent sample data set for years 2013–2014 (training data) and on an additional data set (validation data) of $h(t)$ and $Q(t)$ measurements for years 1978–1979 from hydroscope [26]. In the validation process, a model simulation with 2000 iterations was performed for each of the two sample data sets, in order to achieve the best fit of the regression and test the stability of the models by taking into account the average fit, the R^2, the RMSE, etc., for the training and the validation data.

3. Pinios River basin and study section's (Giannouli, Larissa) geomorphology and geology

The Pinios River is the third longest river in Greece and the biggest river in Central Greece which forms its basin mainly at the eastern part of Central Greece and drains the entire hydrologic basin of Thessaly, discharging its flows into the Aegean Sea at Messagala,Stomio area, where its delta is formed. The Pinios River derives at the north-western part of the Thessaly plain, from the confluence of Ion and Malakasiotis Rivers [27–29]. It is surrounded by mountainous areas which enclose its drainage basin and form its watershed. To the north are the Titaros Mt. (1,837 m) and the Kamvounia Mt. (1,615 m), to the north-east are the Olympos Mt. (2,917 m) and the Ossa Mt. (1,978 m), to the east is the Pilio Mt. (1,548 m), to the south is the Orthrys Mt. (1,726 m) and, finally, to the west are the Pindos Mt. (2,204 m) and the Koziakas Mt. (1,901 m). Internally, the plain is divided by a low-lying hill area into a western part (Trikala–Karditsa) and an eastern part (Larissa) [27,28,30]. The major tributaries of the Pinios River are the Portaikos, Pamisos and Enippeas Rivers to the south-west and the Lithaios, Neochoritis and Titarisios to the north, which all drain large, geologically heterogeneous areas, through extensive hydrographic networks. The total surface area of the Pinios River Basin is 10.550 km^2 (including the drainage basin of the former Lake Karla (about 1.050 km^2)). The basin lies in an area of intense agricultural activities. The cultivated land covers 477,781 ha from which 265,544 ha are irrigated. The participatory irrigation projects cover approximately 35–40% of the irrigated land and the private projects 60–65%, respectively. A significant variety of irrigation systems exist with characteristic advantages for certain soil/climatic conditions as well as for crop requirements.

The Pinios River crosses various geotectonic environments, which form the tectonic window of the Olympos–Ossa unit, the Koziakas unit and the eastern nappes of the Pelagonian zone and the Eastern Greece zone (Subpelagonian) [29,31,32]. The study section at Giannouli monitoring station is located near the main Thessalian city of Larissa. In this section, the sinuosity of the river ranges from 1.77 to 1.83. The type of meandering river bed can be seen throughout the section, while mainly fine coarse sediment are transported and deposited by the river [28]. The river type is mainly meandering with an active river bed width 60–80 m (mean value (mv) 70 m) and a broad width 80–140 m (mv 100 m). There is one river terrace having width of 200–1,600 m (mv 650 m) and which is located 8 m above the river bed. The river bed slope (%) is about 0.06 and the river bed granulometry consists of sands, mud and gravels of various sizes. The geologic substrate of the area is mostly Plio-Pleistocene to Holocene sediments. The Giannouli, Larissa section's geometry modelling results showed that the river width fluctuated during the measurement period between 7.90 and 64.52 m (mean = 29.593, Std D = 19.148). The net river width fluctuated between 7.90 and 57.32 m (mean = 25.821, Std D = 16.096). The flow area of the section ranged from a minimum 8.87 to a maximum 138.52 m^2 (mean = 40.179, Std D = 33.605). The wetted perimeter also fluctuated accordingly from a minimum 11.03 to a maximum 82.30 m (mean = 33.642, Std D = 22.763). The minimum water depth fluctuated between 0.00 and 0.42 m (mean = 0.180, Std D = 0.119). The maximum water depth was found between 1.50 and 4.77 m (mean = 2.556, Std D = 0.802). In some cases, extreme streamflow brought debris to Giannouli, Larissa section which resulted in the accumulation of tree trunks and branches at bridge's columns.

4. Results and discussion

4.1. Rainfall vs. discharge analysis, environmental flows and irrigation management

The rainfall data of the Giannouli, Larissa area were processed for years 2013–2014 and 1978–1979, and in conjunction with dates of measurements and $Q(t)$ data of the present study and also historical data [26] are depicted in Fig. 1(a) and (b).

The annual rainfall (precipitation) of years 2013 and 2014 was 331.60 and 427.00 mm, respectively. The

mean monthly precipitation for the years 2013 and 2014 was found to be 27.63 and 35.58 mm, respectively. A significant increase of 28.77% to annual and mean monthly precipitation occurred between the two years. The annual rainfall of year 1978 and 1979 was 613.70 and 507.80 mm, respectively. A reduction of 17.26% to annual precipitation occurred between the two years. Moreover, comparison of rainfall between 1978–2013 and 1979–2014 resulted in differences of −45.97 and −15.91%, respectively. The mean monthly river discharges of years 1978, 1979 and 2014 were found to be 35.91, 57.52 and 50.37 $m^3 s^{-1}$, respectively. It was observed (Fig. 1(a) and (b)) that the summer and autumn months (June–October) of recent and also July–September of historic years presented low to zero discharges, which are below the estimated environmental flow upper (safe) limit or EFUL (16.31 and 15.13 $m^3 s^{-1}$ for 2013–14 and 1978–79, respectively) and even below the environmental flow lower (critical) limit or EFLL (10.00 and 9.28 $m^3 s^{-1}$ for 2013–14 and for 1978–79, respectively) [30] of the Pinios River. This environmental risk state (river discharges below EFLL) is due to low summer input flows, low to zero summer rainfalls, demanding agricultural management (extreme river water withdrawals for irrigation purposes) and it must be taken care of with proper environmental and agricultural management and emergency policy measures in order to protect the riverine environment. The Spearman's rho statistical test between the discharge $Q_{(2013–2014)}$ and 2013–2014 rainfall datasets for daily, 2-day moving average, 3-day moving average and 10-day rainfall, resulted in medium and low correlation coefficients of 0.444, 0.490, 0.502 and 0.150, respectively. This is indicating that beyond rainfall, there are other factors influencing the Pinios River velocity and discharge such as flows from: mountainous water springs, tributaries, snow melting and shallow groundwater contributions.

In Thessaly region, the agricultural sector is the main consumer of water (total annual water demand of 1.5–2.0 × 10^9 m^3), which approximately accounts for 95% of the total demands of the region. The irrigated land of the region covers about 265,544 ha. Arable crops of the area exhibit the highest irrigated percentage, followed by fruit trees, vegetables and the vines in a decline order [30]. The River Pinios is

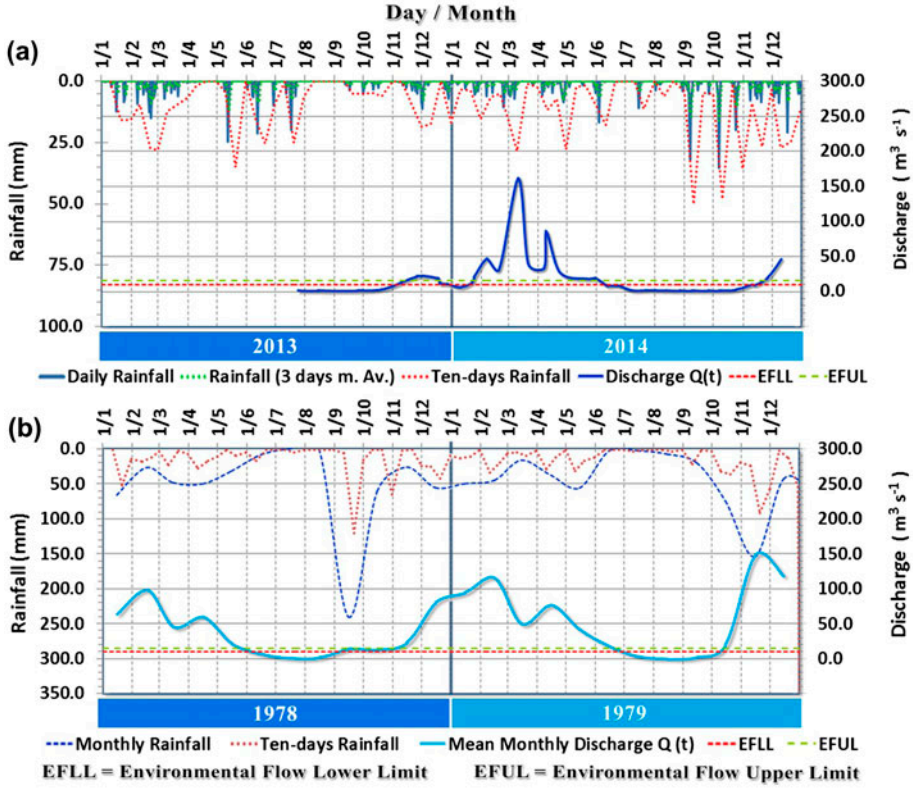

Fig. 1. (a) Daily Rainfall, 3 d moving average rainfall, ten-days rainfall and discharge's variation curve, for measurement dates in 2013–2014 and (b) monthly Rainfall, ten-days rainfall and mean monthly discharge variation curve in 1978–1979, with environmental flows curve limits.

contributing to the agricultural sector with its flows used mainly for irrigation purposes. However, the extreme river water withdrawals for irrigation purposes are disrupting river's good state. The hydrological and RC modelling, the extrapolated parts, the rainfall vs. discharge and environmental flows analysis, the river bed variation analysis and the hydraulic properties estimates are aiming and proposed to serve as hydrological assisting tools for environmental water resources and irrigation management in the wider Giannouli, Larissa area. These assisting tools will help water authorities accurately and quickly estimate river's water quantities and variation with a minimum cost and effort, and they could be used for irrigation management, environmental flow estimation, groundwater recharge, flood protection and other purposes.

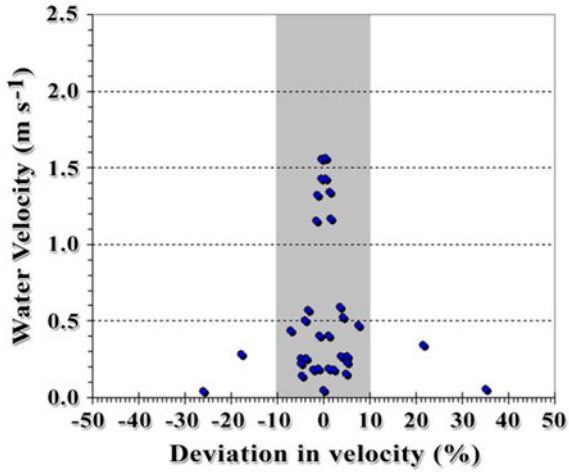

Fig. 2. Trends of water velocity deviations. Shading indicates those velocity deviations within ±10%.

4.2. Hydrological and RC modelling

Following the hydro-measurements protocol [33,34], after each pair of sequential velocity measurements, a percentage check was performed to obtain the deviation in velocity (%) between the measurements. The acceptable deviation of the protocol was within ±10% according to ISO 748:2007 [34], between a pair of sequential velocity measurements for all verticals of the river cross-section. Any velocity measurement results beyond the ±10% deviation were rejected, and a new pair of velocity measurements was taken. An example of velocity measurement results (December 2014) is given in Fig. 2, where shading indicates those velocity deviations within ±10%. The velocities outside of the shaded area were rejected as not acceptable according to ISO 748:2007 [34].

Then, for each measurement date, the Froude number was calculated. This was performed by taking into account the following: (a) velocity measurements at cross-section's segments according to the hydro-measurements protocol and ISO 748:2007 [33,34], (b) acceptable velocity's deviation in each segment, (c) the calculated average velocity V (m s^{-1}) of the streamflow measurements at the specific river section, (d) the acceleration due to gravity g = 9.81 (m s^{-2}) and (e) the characteristic length L (m) for the particular type of open channel.

In open-channel hydraulics, Froude number (Fr) is a very important non-dimensional parameter that provides the ratio of inertia force on an element of fluid (in our case water) to the weight of the fluid element, i.e. the inertial force divided by gravitational force [5,6]. The value of the Froude number provides information about the type of the flow. In particular, the Froude number (Fr) is considered valuable since its value for any particular open-channel flow, provides information on whether that flow is subcritical (Fr < 1), critical (Fr = 1) or supercritical (Fr > 1) flow. Moreover, when Froude number is 1, the velocity is equal to the velocity of wave propagation, or celerity. When this condition is attained, downstream wave or pressure disturbances cannot travel upstream.

The results and statistical analysis showed that Fr during the measurement period is oscillating from a minimum 0.109 to a maximum 0.283 (mean Fr = 0.172, standard deviation Std D = 0.0406), as illustrated in Table 2.

The open-channel flow water measurement (like in river Pinios), generally requires that the Froude number, of the approach flow be less than 0.500 to prevent wave action that would hinder or possibly prevent an accurate head reading [6,9,10] for stage. The above-mentioned Fr results of the present study are ranging bellow the limit 0.500 in a subcritical flow, so it is most probable that the accuracy of our measurements readings have not been affected.

Statistical analysis results showed that the minimum water depth fluctuated during the measurement period between 0.00 and 0.42 m (mean = 0.180, Std D = 0.119). The maximum water depth fluctuated between 1.50 and 4.77 m (mean = 2.556, Std D = 0.802), see Table 2. The segment's maximum water velocity measured from a minimum 0.452 to maximum 1.693 m s^{-1} (mean 1.247, standard deviation Std D = 0.348). In detail, the results of the statistical analysis [17–21] of various hydrological variables and hydraulic properties (measured and calculated) at Giannouli, Larissa's station (P145), are presented in Table 2.

The results of river bed variation, defined by geometric shape, river width, net river width, mean water

Table 2
Results of the statistical analysis (descriptive statistics), for the various hydrological variables and hydraulic properties (measured or calculated) for Giannouli, Larissa station (P145)

Variable	*N*	Range	Min	Max	Mean	Std. Deviation	Variance
Stage *Hcor* (datum corrected)	18	2.42	1.550	3.970	2.488	0.556	0.309
Discharge measured	18	158.91	3.148	162.059	32.522	38.138	1,454.484
Segment's water velocity measured min	18	0.98	0.030	1.013	0.224	0.262	0.069
Segment's water velocity measured max	18	1.24	0.452	1.693	1.247	0.348	0.121
Mean water velocity max of verticals	18	1.23	0.450	1.683	1.208	0.374	0.140
Mean water velocity *V*m of flow area	18	0.88	0.287	1.170	0.705	0.232	0.054
Depth min	18	0.42	0.000	0.420	0.180	0.119	0.014
Depth max	18	3.27	1.500	4.770	2.556	0.802	0.644
Mean depth min	18	0.54	0.265	0.805	0.499	0.147	0.022
Mean depth max	18	3.24	1.430	4.670	2.371	0.716	0.513
Water mean depth	18	1.24	1.073	2.316	1.356	0.299	0.089
River's width	18	56.62	7.900	64.520	29.593	19.148	366.650
Net river's width	18	49.42	7.900	57.320	25.821	16.096	259.086
Measured depths	18	18.00	5.000	23.000	13.944	6.708	44.997
Flow area	18	129.64	8.871	138.516	40.179	33.605	1,129.304
Wetted perimeter	18	71.27	11.030	82.296	33.642	22.763	518.169
Hydraulic radius	18	0.88	0.804	1.683	1.147	0.206	0.043
Hydraulic depth	18	1.35	1.118	2.465	1.467	0.322	0.104
n Manning coefficient of roughness	18	0.19	0.048	0.235	0.084	0.043	0.002
Discharge calc	18	158.91	3.148	162.059	32.522	38.138	1,454.484
Velocity calc	18	0.88	0.287	1.170	0.706	0.231	0.054
Froude number	18	0.17	0.109	0.283	0.172	0.041	0.002

depth, flow area, wetted perimeter, hydraulic radius, hydraulic depth and *n* Manning coefficient of roughness presented a remarkable variation (see Table 2) during the study period. In Fig. 3(a) and (b) are presented the river bed topology, the river width, the water depth (as elevation), the water flow area (in blue colour), the bed in grey colour and the wetted perimeter observed on 23 October 2013 and on 11 March 2014: the first date is the one with the minimum river width (7.90 m) and net river width (7.90 m) and minimum discharge Q (3.148 $m^3 s^{-1}$), while the second date is the one with the maximum river width (64.52 m), maximum net river width (57.32 m) and maximum discharge Q (162.059 $m^3 s^{-1}$) for the study period. In Fig. 3(c) and (d) are shown representative diagrams of modelled river water's velocity vertical profiles vs. depth in percentage of total water depth, from measured and estimated water velocity data for the two river cross-sections observed on the above-mentioned dates.

In Fig. 3(e), representative photos of the Pinios River and measurements' process are shown. Variation in results between the two dates, for Froude number is due to different mean velocities, flow areas and geometric shapes. Variation in results between the two dates for *n* (Manning's coefficient of roughness) is due to different channel conditions, mean velocities, wetted perimeters, flow areas and geometric shapes.

On 23 October 2013 (Fig. 3(a)), the river bed is characterized as pool–small riffle bed system, irregular meandering channel with medium to deep pool with boulders with lower mean water velocity (0.368 m s^{-1}) and subcritical flow (Fr = 0.1109). On 11 March 2014 (Fig. 3(b)) the river bed is characterized as irregular channel cross-section with meanders, riffle bed system, irregular meandering channel with deep pools with boulders (*n* Manning's coefficient of roughness = 0.0563) with higher mean water velocity (1.091 m s^{-1}) and subcritical flow (Fr = 0.2241).

In the final stage of modelling, the river flow RC and the river bed variation of the Pinios River at Giannouli, Larissa monitoring point were modelled using a regression statistical analysis [21,35–37] with dependent variable the discharge $Q(t)$ ($m^3 s^{-1}$) and independent variable the stage *Hcor(t)* (m) [datum corrected], in order to identify the best fit model for the compilation of the RC for years 2013–2014 $h(t) - Q(t)$ data set. The RC is generally calibrated over a series of $h(t) - Q(t)$ pairs, where $h(t)$ is the water level measured at time t and $Q(t)$ is the concurrent river discharge, which, in turn, is often estimated through the velocity–area method [38,39]. Even though $Q(t)$ values are not direct

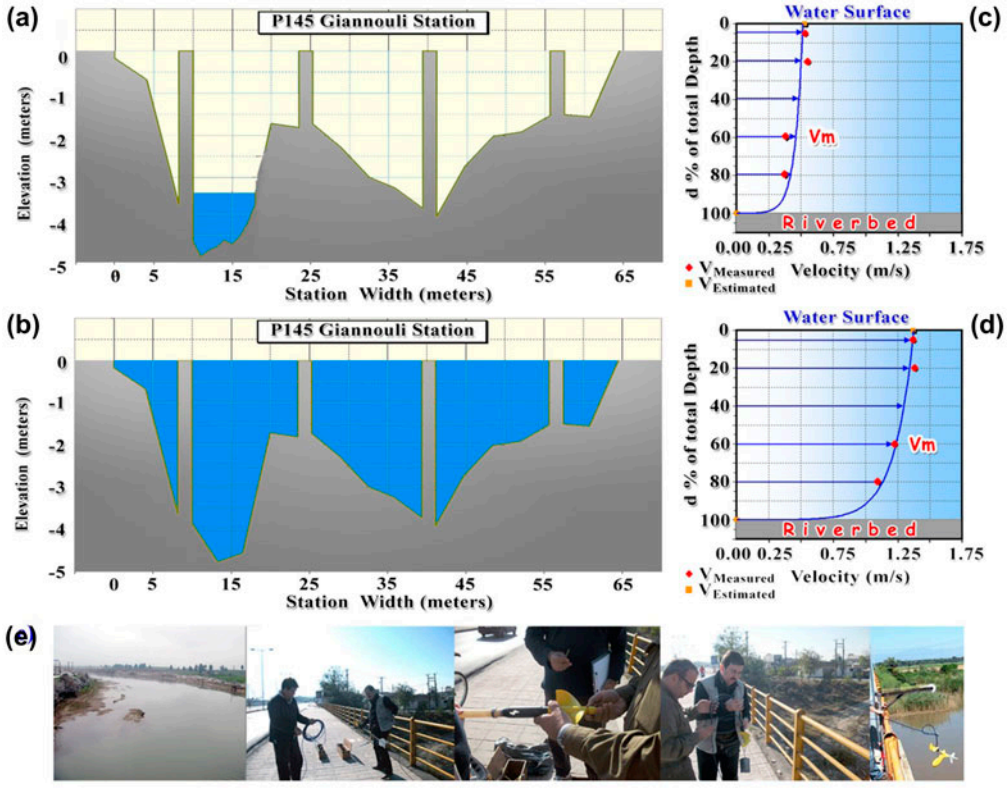

Fig. 3. (a, b) River bed topology cross-sections at P145 for (a) 23 October 2013 and (b) 11 March 2014, (c, d) Diagrams of modelled water's velocity vertical profiles vs. depth [% of total water depth] for (c) 23–10-2013 and (d) 11–03-2014, and (e) Representative photos of Pinios River and measurements' process.
Source: Photographic images reproduced with permission.

measurements, but rather estimates of the real and unknown discharge values, they are seldom associated with a statement of their uncertainty in practical applications [40].

The most commonly used stage–discharge ratings, treats the discharge as a unique function of the stage. These ratings typically follow a power low curve of the form given by Eq. (4) [12,19,38,41]:

$$Q = c\,(h - a_0)^{b1} \tag{4}$$

where Q is the discharge, h is the stage and c, a_0, $b1$ are the calibration coefficients: c is the discharge when the effective depth of flow $(h - a_0)$ is equal to 1; a_0 is the gauge height at zero flow; $b1$ is the slope of the RC; $(h - a_0)$ is the effective depth of water on the control.

Instead of Eq. (4), other models have been used for stage–discharge ratings [9,10,38]. In the present study, using the $h(t) - Q(t)$ data set pairs measurements, eight different model equations (linear, logarithmic, inverse, compound, power, growth, exponential and logistic type) were modelled and tested in order to investigate which is the best to represent the physical phenomenon for Giannouli, Larissa monitoring station. Evaluation of the best model was based on the quantitative results as evaluation criteria [27,36,42–44] of the statistical analysis. Quantitative research leads to a generalization of results and supplies relatively standardized information [27,36,45,46]. The quantitative results of statistical analysis for model summary (R^2, F test for best fit and significance) and parameter estimates (Constant c and Regression coefficient $b1$) regarding modelling [9,21,27,35,36,47], of the streamflow's RC for years 2013–2014 are presented in Table 3. The coefficient of determination (R^2) is an indicator of the variance proportion of the dependant variable [21,27,35,36] which in our case is discharge $Q(t)$ and can be explained by the variation in the independent variable (measured stage $h(t)$). A good or high coefficient of determination (above 0.80 or 0.95) can possibly indicate that the independent variable (stage $Hcor(t)$) has a significant effect on the prediction of the water discharge $Q(t)$.

Analysing the statistical results of the 8 tested models (Table 3), we observe that the models

Table 3
Statistical analysis results of the various models' equations, summary and parameter estimates

S. no.	Model	Equation	Model summary			Parameter estimates	
			R^2	F	Sig.	Constant c	Regression coefficient $b1$
1	Linear	$Q = b1\ (h - a_0) + c$	0.8810	118.500	0.000	−127.6363	64.364
2	Logarithmic	$Q = b1\ \ln(h - a_0) + c$	0.7693	53.357	0.000	−107.4920	157.364
3	Inverse	$Q = c\ (b1/(h - a_0))$	0.6285	27.073	0.000	177.1495	−344.816
4	Compound	$Q = c\ (b1^{\ h-a0})$	0.9167	176.178	0.000	0.2894	5.518
5	Power	$Q = c\ (h - a_0)^{b1}$	0.9504	306.627	0.000	0.3540	4.5502
6	Growth	$Q = e^{(c\ +\ b1\ (h\ -\ a0))}$	0.9167	176.178	0.000	−1.2401	1.708
7	Exponential	$Q = c\ (e^{(b1\ (h\ -\ a0))})$	0.9167	176.178	0.000	0.2894	1.708
8	Logistic	$Q = (1/u + c\ b1^{(h\ -\ a0)})$	0.8864	124.906	0.000	121.755	0.036

Notes: Dependent variable: Discharge Q ($m^3\ s^{-1}$), independent variable: Stage $Hcor = (h - a_0)$ (m) with h = the stage which is the water level above a vertical reference, a_0 = stage at zero discharge, ln = the natural logarithm, c = a constant, $b1$ = Regression coefficient, u = model's upper bound value.

exponential, growth and compound have exactly the same $R^2 = 0.917$. This is statistically possible [21,35] and is due to the similar exponential form of their equations [21,35,36] that yields the same regression coefficients ($b1$) for the exponential and growth models and in the same c constants for the exponential and compound models, which in combination with the regression's c and $b1$ best values resulted in the same final R^2 and curves for the above-mentioned three models.

In Fig. 4(a), the graphical representations of the resulted RCs of years 2013–2014 data set for the studied models (a) linear, (b) logarithmic, (c) inverse, (d) compound, (e) power, (f) growth, (g) exponential and (h) logistic are presented.

The results of the best model (power) curve fit of stage $Hcor(t)$ (m) vs. water discharge $Q(t)$ ($m^3\ s^{-1}$) is depicted in Fig. 4(b). In the same figure, it is observed that the data values (dots) are within the 95% confidence space limits, a fact which indicates that there are not any data outliers that could have a negative effect on curves modelling. The measurement per cent difference, D(%) between the measured discharge [$Qm(t)$] and the RC discharge [$Qr(t)$] (predicted values) was calculated according to Sauer [48], for each model and each measurement case.

The results of D(%), for measurements cases of years 2013–2014 are presented in Fig. 5(a). Essentially, this is the percent difference between the measured discharge $Qm(t)$, and the RC discharge $Qr(t)$ (that is the calculated $Q(t)$ from each model), which corresponds to the stage height of the discharge measurement. It is observed that the power model has minimum measurement percent differences. Moreover, the standard error of estimates (SEE) of the studied models is depicted in Fig. 5(b).

The overall performance of the various data-driven models was evaluated by means of the following errors statistics criteria (esc): (a) RMSE, (b) coefficient of determination (R^2), (c) SEE, (d) MAE and (e) MAD D(%). The results of the errors statistics criteria are presented in Table 4.

The proposed MPI of each model was calculated using the mathematical Eq. (3) (see Section 2.3). As the value of the MPI approaches one, the better performance of the relative model is obtained. An example of the MPI Index calculation for power model is given below:

for $j = 1$ the esc $\in$ RMSE => $esc_{(RMSE,k)} = esc_{(8.228,1)}$ => $SCesc_{(RMSE,k)} = 20$,

for $j = 2$ the esc $\in R^2$ => $esc_{(R^2,k)} = esc_{(0.9504,1)}$ => $SCesc_{(R^2,k)} = 20$,

for $j = 3$ the esc $\in$ SEE => $esc_{(SEE,k)} = esc_{(0.2277,1)}$ => $SCesc_{(SEE,k)} = 20$,

for $j = 4$ the esc $\in$ MAE => $esc_{(MAE,k)} = esc_{(5.060,1)}$ => $SCesc_{(MAE,k)} = 20$,

for $j = 5$ the esc $\in$ MAD D(%) => $esc_{(MAD\ D(\%),k)} = esc_{(2.191,2)}$ => $SCesc_{(MAD\ D(\%),k)} = 18$.

Then, the MPI for Power model is calculated as follows:

index MPI = $[(SCesc_{(RMSE,k)} + SCesc_{(R^2,k)} + SCesc_{(SEE,k)} + SCesc_{(MAE,k)} + SCesc_{(MAD\ D(\%),k)})]/100$ => index MPI = $[(20 + 20 + 20 + 20 + 18)]/100$ => indexR MPI = 0.980.

Based on the results of esc, on the classification of each criterion and on the proposed MPI calculated as above, the models tried are ranked in descending order as follows: (1) power, (2) logistic, (3) linear, (4) compound and growth and exponential, (5) logarithmic and (6) Inverse.

Based on the parameters measurements and the above model classification, the resulted power model (Eq. (5)) was selected as the best model (RMSE = 8.228,

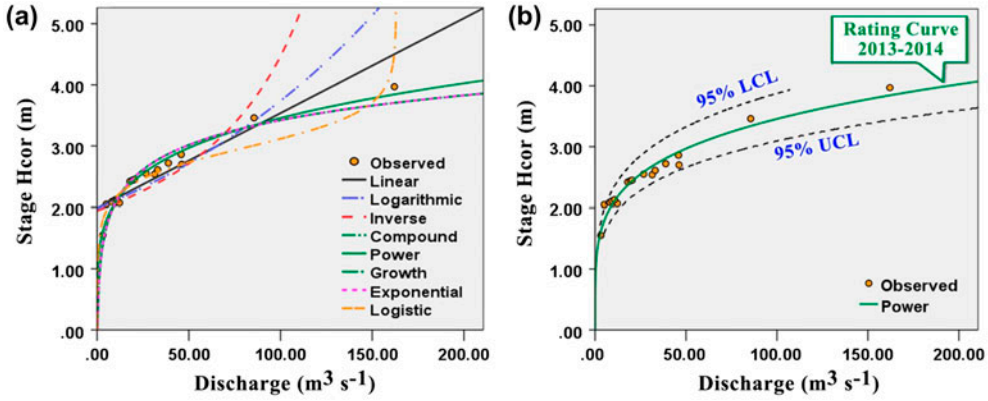

Fig. 4. (a) RCs for years 2013–2014: Stage $Hcor = (h - a_0)$ (m) vs. Discharge Q ($m^3\ s^{-1}$) for the 8 studied models and (b) Final RC with 95% confidence limits curves (95% UCL and 95% LCL) for years 2013–2014 data set calculated with the power model.

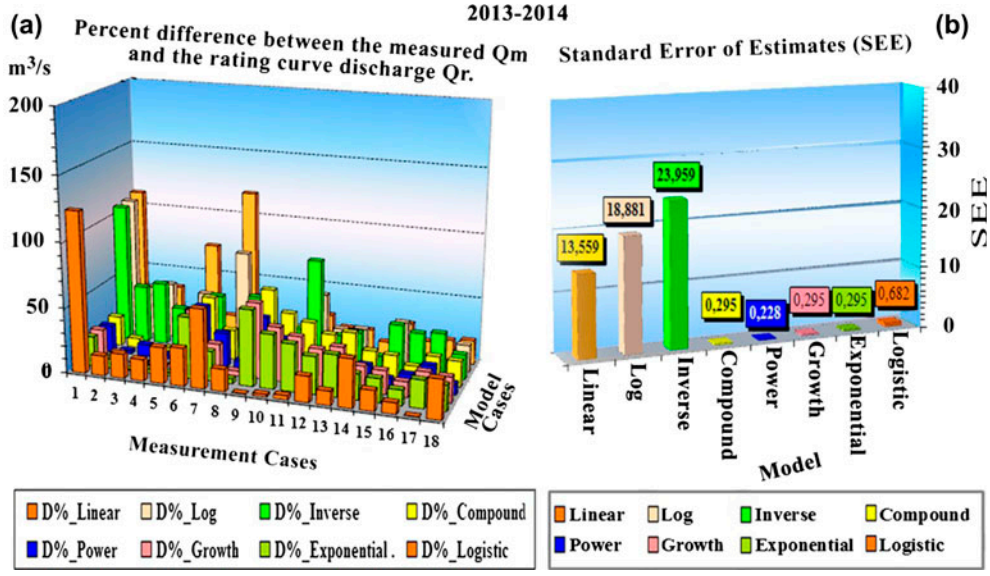

Fig. 5. Results of 2013–2014 $h(t) - Q(t)$ data: (a) MAD D(%) between the measured discharge [$Qm(t)$] and the RC discharge [$Qr(t)$] (predicted values) and (b) Standard Error of Estimates of the studied models.

Table 4
Models' overall performance results of the errors statistics criteria and MPI index

S. no.	Model	RMSE	R^2	SEE	MAE	Mean MAD D(%)	MPI index	Overall performance rank (Class)
1	Linear	12.783	0.8810	13.5587	8.919	2.110	0.810	3
2	Logarithmic	17.802	0.7693	18.8814	11.352	12.500	0.575	5
3	Inverse	22.589	0.6285	23.9594	14.436	23.494	0.470	6
4	Compound	23.187	0.9167	0.2951	10.139	3.746	0.720	4
5	Power	8.228	0.9504	0.2277	5.060	2.191	0.980	1
6	Growth	23.187	0.9167	0.2951	10.139	3.746	0.720	4
7	Exponential	23.187	0.9167	0.2951	10.139	3.746	0.720	4
8	Logistic	13.209	0.8864	0.6817	6.597	2.696	0.820	2

R^2 = 0.9504, Adjusted R^2 = 0.9749, SEE = 0.2277, MAE = 5.060, Mean MAD D(%) = 2.191 and MPI = 0.980) to use for the compilation and best fit of the streamflow RC (Fig. 4(b)) at the studied monitoring station. The power model (Eq. (5)) expresses streamflow $Q(t)$ and it is the best approximation for the recent time period 2013–2014 of $h(t) - Q(t)$ data series for curve's ($RC_{(2013–2014)}$) best fit, so far.

$$Qr = c(h - a_0)^{b1} = 0.3540 * (h - a_0)^{4.5502} (\mathrm{m^3\,s^{-1}}) \quad (5)$$

where Qr is the discharge ($m^3\,s^{-1}$); h is the stage which is the water level above a vertical reference and a_0 is the level corresponding to zero flow rate above the same reference, while numbers 0.3540 and 4.5502 are the equation's parameters (calibration coefficients). The first is the c constant, while the second one is the regression coefficient $b1$.

The developed $RC_{(2013–2014)}$ of the present study, in our knowledge, is considered to be the best approximation of recent years $h(t) - Q(t)$ data series for curve's best fit so far at the Giannouli, Larissa study area in comparison to previously developed RCs.

Hatzigiannakis et al. [9] and Hatzigiannakis et al. [10] developed RCs for the study area. These curves in comparison with the one of the present study have the following cons: (a) a smaller or marginal sample N [9,10], for RC modelling according to ISO 1100-2 [12], (b) a limited maximum discharge $Qmax$ [9], (c) lower R^2 results [9,10] which although are still considered to be very good R^2, they are not classified as high coefficients of determination, as the one achieved in the present study, (d) higher standard errors of estimates (SEEs) [9,10] and the rule for SEE is the lower the better, so SEE of the present study is considered as a better one, (e) higher MAD D(%) than the one of the present study and the rule for MAD D(%) is the lower the better.

Moreover, in the previous mentioned studies, neither an RC extrapolation was performed, nor a model's validation, which is an essential part of the modelling process. The modelling aim is to validate the goodness of fit of the model in order to ensure that the $h(t) – Q(t)$ data series fitting is satisfactory and that also the stability of the developed relationship is adequate. These parts of the modelling process of the present study are presented in the following paragraphs.

Conclusively, in natural rivers, the $h(t) - Q(t)$ relationship in general appears to be a loop, rather than single valued. The results showed that the compiled streamflow RC of the Pinios River appears to have an adequate relationship especially for power model and secondarily for logistic, linear, compound, growth and exponential models.

4.3. Extrapolation modelling of the RC

Extreme importance is given to the capability of the stage–discharge relation to be applicable for extreme flow conditions. Discharge measurements are usually missing in the definition of the upper part and lower end of the RC. The extrapolation of $h(t) – Q(t)$ data series used for the modelled RC, are subject to errors that can have significant implications for flood management (upper extrapolated part of the curve) and for water resources planning and management (lower extrapolated part of the curve). Unfortunately, discharge measurements that cover the upper and lower ends of the RC often are lacking, so, ratings often are extrapolated in order to estimate streamflow outside the range of observations. For the extrapolation of the RC, in international bibliography and standards, it is noted that a stage–discharge relation should not be applied outside the range of discharge measurements upon which it is derived. If estimates of flow, however, are required outside the range, it may be necessary to make an extrapolation of the RC [12–14,41], taking into account as an advice that "the rating should not be extrapolated beyond 1.5 times [12–14] or twice the largest measured discharge except as a last resort" [41].

In the hydrometric practice of the present study by examining bibliography, it has been observed that during the event of a large flood [27,37,49–51], it is impossible or impractical to measure velocity directly [9,10,13,27] in order to calculate streamflow discharge. It seems that more often than not, the flood stage in a given time instant goes beyond the range of the data used to define the river flow RC [9,10]. For this reason the extrapolation of the curve is needed when water level of the river bed is recorded below the lowest or above the highest level, which were used for the compilation of the initial curve. Also, extensive errors can result if the functional form of a power model RC (as $Q = c\ (h - a_0)^{b1}\ (\mathrm{m^3\,s^{-1}})$) is extrapolated beyond the actual range of measured discharges without consideration of the cross-section geometry and the effective roughness. Moreover, the graphical extension of curve or by the fitted $h(t) - Q(t)$ relationship is adequate only for a small extension. The conveyance-slope method is the most common method used nowadays for RC extrapolation. However, this method assumes that the geometry of the cross-section used for discharge measurements is fairly representative of that of a long reach of the downstream channel. Unfortunately, the need to meet this assumption

eliminates from consideration the discharge measurements that are made at constricted cross-sections (at bridges) of gauging stations. So, our monitoring gauging station with the cross-section at the bridge of Giannouli, Larissa does not meet the above assumption and the use of conveyance-slope method is rejected.

A logarithmic extrapolation $Q = b1\ \ln(h - a_0) + c$ ($m^3\ s^{-1}$), is particularly suited to channel control conditions for medium and high flows, but should probably never be used to extrapolate more than about 1.5 times [12,14] or twice [41] the highest measured discharge. A logarithmic extrapolation (Fig. 6) was performed based on the final RC. In the upper part of the curve, extrapolation consisted of two subparts: the first one was 1.5 times and the second one was 2 times the highest measured discharge for the time period 2013–2014.

The extrapolation parts are noted in the diagram (Fig. 6) with "Ext", "Ext-1.5x" and "Ext-2x", on red areas and red limit dashed lines and they are ranging on discharges from 0.01 to 3.15 ($m^3\ s^{-1}$) (low discharges) and from 162.06 to 243.09 ($m^3\ s^{-1}$) (medium discharges) which is 1.5 times the highest measured discharge according to ISO 1100-2:1998 [12,14] and from 243.09 to 324.118 ($m^3\ s^{-1}$) (high discharges) which is 2 times the highest measured discharge according to Rantz et al. [41].

It is particularly suited to channel control conditions for medium and high flows. Low flow extrapolation of a RC is often required in the management of surface water resources and in their supply for domestic, industrial, agricultural or environmental uses. Unfortunately, there is no assurance that the extrapolation of the RC for low flows is precise, but the extrapolation shown in Fig. 6 seems to be a reasonable one. In order to acquire that assurance with statistical confidence and validate the lower extrapolation part of the RC, accurate low flow discharge (from 0.100 to 3.148 ($m^3\ s^{-1}$)) and stage measurements are required.

Regarding the upper extrapolated curve part, it is noted that RCs, very often must be extrapolated beyond the range of measured high discharges either for estimating flood discharge that are not measurable from measured stage, or to estimate the height or level corresponding to high return period floods, calculated by numerical models for flood warning and protection. The upper extrapolation of the $RC_{(2013–2014)}$ at the "Ext-1.5x" part although it is underestimating the data is very close to the $RC_{(1978–1979)}$ curve. When the extrapolation goes within the "Ext-2x" part, it is also underestimating the data, and the higher in $Q(t)$ the extrapolation is, the higher the departure from the $RC_{(1978–1979)}$ curve is. It is concluded that for the Giannouli, Larissa monitoring station the rating should not be extrapolated beyond 1.5 times the largest measured discharge. Nevertheless, large element of uncertainty always exists in the extrapolation modelling process of the upper extrapolated curve part. It must be noted that the graphical representation with arithmetic scales instead of logarithmic is convenient to use and easy to read. Arithmetic scales are ideal for displaying a RC, and have an advantage over logarithmic scales, in that zero values of gauge height and/or discharge can be plotted in the diagram. So, often in practice, except the logarithmic extrapolation and the presented logarithmic diagram (Fig. 6), a conventional arithmetic scale diagram is developed for presentation purposes, for plotting the zero values of gauge height and/or discharge measurements (see Fig. 9). However, for analytical purposes, arithmetic scales have practically no advantage over logarithmic scales. A stage–discharge model on arithmetic scales is almost always a curved line, concave downwards, which in most cases could be quite difficult to shape correctly if only a few discharge measurements are available. Fortunately, this is not the case in the present study. Although, a large sample data set is not available, the sample size $N = 18$ is consider to be an adequate one and it is above the appropriate and ISO recommended minimum sample limit of $N = 15$ for RC modelling according to ISO 1100-2 [12]. The extrapolated part of the RC should be used in cases where high flows occur in the Pinios River and it is very difficult or impossible to measure the streamflow discharges during the flood events.

4.4. Model's validation

Model validation, model selection and error estimation [22–25] is a crucial part of the study and it was based on two separate parts. In the first part, the cross-validation method was fully applied on data, based on the existing sample data set with the $h(t)$ and $Q(t)$ measurements for years 2013–2014. In the second part, the validation method between two sample datasets was fully applied on the existing sample data-set with $h(t)$ and $Q(t)$ measurements for years 2013–2014 and on an additional data set (validation data) with $h(t)$ and $Q(t)$ primary data for years 1978–1979 from hydroscope [26]. Validation results were analysed, compared and discussed.

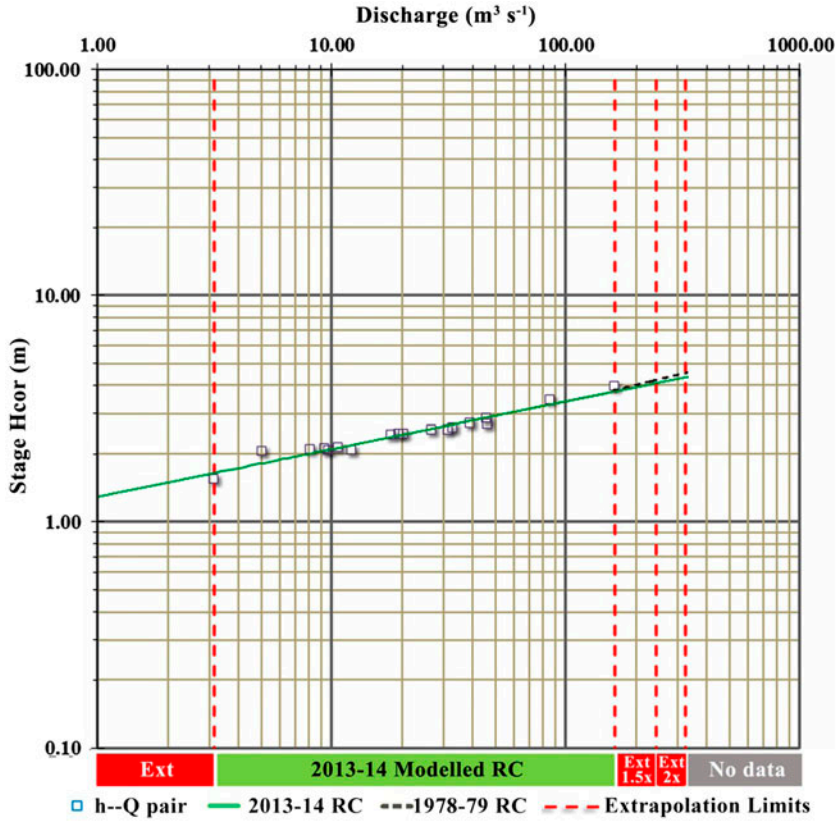

Fig. 6. A logarithmic extrapolation based on the final RC.

4.4.1. Cross-validation method

As noticed in the early 30s by Larson [52], training an algorithm and evaluating its statistical performance on the same data yields an overoptimistic result. Cross-validation (CV) statistical method was raised to fix this issue, starting from the remark that testing the output of the algorithm on new data would yield a good estimate of its performance [23,24,53]. CV is a popular strategy for algorithm selection. The main idea behind CV is to split data, once or several times, for estimating the risk of each algorithm: part of data (the training sample) is used for training each algorithm and the remaining part (the validation sample) is used for estimating the risk of the algorithm. Then, CV selects the algorithm with the smallest estimated risk [22].

The major interest of cross-validation lies in the universality of the data splitting heuristics. It only assumes that data are identically distributed, and training and validation samples are independent, which can even be relaxed. Therefore, crossvalidation can be applied to (almost) any algorithm in (almost) any framework, such as regression [23,24], density estimation [54,55] and classification [25,56] among many others. A cross-validation analysis [22–24] was performed in order to validate the regression modelling analysis [23,24] of $h(t)$ and $Q(t)$ measurements and its best fit model (power model) and analyse the error statistics criteria of each sample case for all models [25] and also, the proposed MPI. The leave-one-out (LOO) method [22] was used in conjunction with a developed cross-validation statistical rule script in SPSS software [21] to test the cross-validation hypothesis. According to Breiman and Spector [57], the best risk estimator is LOO. The results of the cross-validation analysis for model selection and error estimation showed that the data fitting of the selected power model is very satisfactory and the stability of the developed relationship (Eq. (5)) is robust as indicated by the statistical (Table 4) and also by the graphical results in Fig. 7(a)–(d). In these figures are depicted the results of the various models' criteria: RMSE vs. cross-validation's sample case (Fig. 7(a)), R^2 vs. cross-validation's sample case (Fig. 7(b)), SEE vs. cross-validation's sample case (Fig. 7(c)) and the results of the MAE vs. cross-validation's sample case (Fig. 7(d)).

The results showed that the power model yielded the best esc values in most of the cross-validation's sample cases (17 of total 18) and the best model stability.

By observing Fig. 7(a)–(d), it can be seen that the pattern of the employed statistical criteria it looks similar but it is not exactly the same. The diagrams of the various model's error statistics criteria results vs. cross-validation's sample case, revealed that in sample cross-validation case 11 the models—logistic, linear, compound, growth, exponential, logarithmic and inverse—are presenting a big improvement in their results values of RMSE, of SEE and of MAE. Moreover, inverse, logarithmic, linear and logistic models are presenting medium improvement in their results values of R^2.

These results on models' errors statistics criteria are due to the fact that the sample case 11 has the maximum discharge *Qmax* (162.059 $m^3 s^{-1}$) observation for the study period and the aforementioned models statistically work better without relative extreme case values and worst with infinity value or extreme case values.

The statistical *t* tests' [21] (for 95% and also for 99% confidence interval of the difference) results on cross-validation, revealed that there is no statistical significant difference between the RMSEs, R^2, SEEs and also between the MAEs of the 18 cross-validation's sample cases for power model, indicating low variability on results of this model and therefore high model stability. The 95 and 99% confidence interval of the difference provides an estimate of the boundaries between which the true mean difference of model's RMSE, R^2, SEE and MAEs lies in 95 or 99% of all possible random samples of the 18 $h(t)$ and $Q(t)$ case measurements for years 2013–2014. These results strengthen the assurance that the stability of the developed relationship (Eq. (5)) is robust with very satisfactory data fitting.

4.4.2. Validation method between two sample datasets

The validation method between two sample datasets was fully applied on the existing sample data set with $h(t)$ and $Q(t)$ measurements for years 2013–2014 (training data) and on an additional data set (validation data) with $h(t)$ and $Q(t)$ measurements for years 1978–1979 from hydroscope [26]. The Spearman's rho statistical test on the two sample datasets resulted in a high correlation between discharges [$Q_{(2013–2014)}$ to $Q_{(1978–1979)}$], with a correlation coefficient = 1.000, and also between stages [$Hcor_{(2013–2014)}$ to $Hcor_{(1978–1979)}$] with a correlation coefficient = 0.967.

In the validation process a model simulation with 2,000 iterations was performed for each of the two sample datasets, in order to achieve the best fit of the regression, taking into account the average fit, the R^2, the RMSE, etc., for the training and the validation data. The outputs of model simulation using 2013–14 data set (training data) and 1978–79 data set (validation data) are depicted in Fig. 8(a) and (b).

The results of model simulation showed that the data fitting of the selected power model is very satisfactory for training and validation data and the stability of the developed relationships (Eqs. (5) and (6)) is robust as indicated by the statistical and also by the graphical results in Fig. 8(a) and (b).

Based on the best fit results the final RCs for training and validation data were developed. In Fig. 9, are depicted the final $RC_{(2013–2014)}$ (modelled with power model) of the present study, the uncertainty curves upper (UCUL) and lower (UCLL) limits for years 2013–2014 data set and the developed $RC_{(1978–1979)}$, (modelled with power model) for years 1978–1979 data set with $h(t)$ and $Q(t)$ primary data acquired from hydroscope [26]. The RC developed with 1978–1979 (historic) data is within the uncertainty space limits of the curve developed with 2013–2014 (recent) data (see Fig. 9), and is very close to the recent years $RC_{(2013–2014)}$.

The RC developed with 1978–1979 $h(t)$ and $Q(t)$ primary data was adjusted for discharge and stage of 2013–2014. This is accomplished so that the discharge of the adjusted 1978–1979 RC represents a recorded stage equal to the discharge from the original recent RC of 2013–2014 that corresponds to the adjusted stage. The time period 1978–2013 over which this occurs is referred to as a period of shifting control. The statistical *t* tests' [21] (with 95% confidence interval of the difference) results on discharge samples (measured and validation data set) revealed that there is no statistical significant difference between esc criteria of the discharges: RMSEs, R^2, SEEs and also between the MAEs of the sample cases (for the power model) indicating that there are not high true differences, between measured and validation data.

Results showed that the power low (Eq. (6)) expresses streamflow $Q(t)$ and it is the best approximation for time period 1978–1979 of $h(t) - Q(t)$ data series for curve's best fit.

$$Qr_{(1978–1979)} = c(h_{adj} - a_{0adj})^{b1} = 0.3115 * (h_{adj} - a_{0adj})^{4.6711} \ (m^3 s^{-1}) \quad (6)$$

where $Qr_{(1978–1979)}$ is the discharge ($m^3 s^{-1}$), h_{adj} is the adjusted stage which is the water level above a

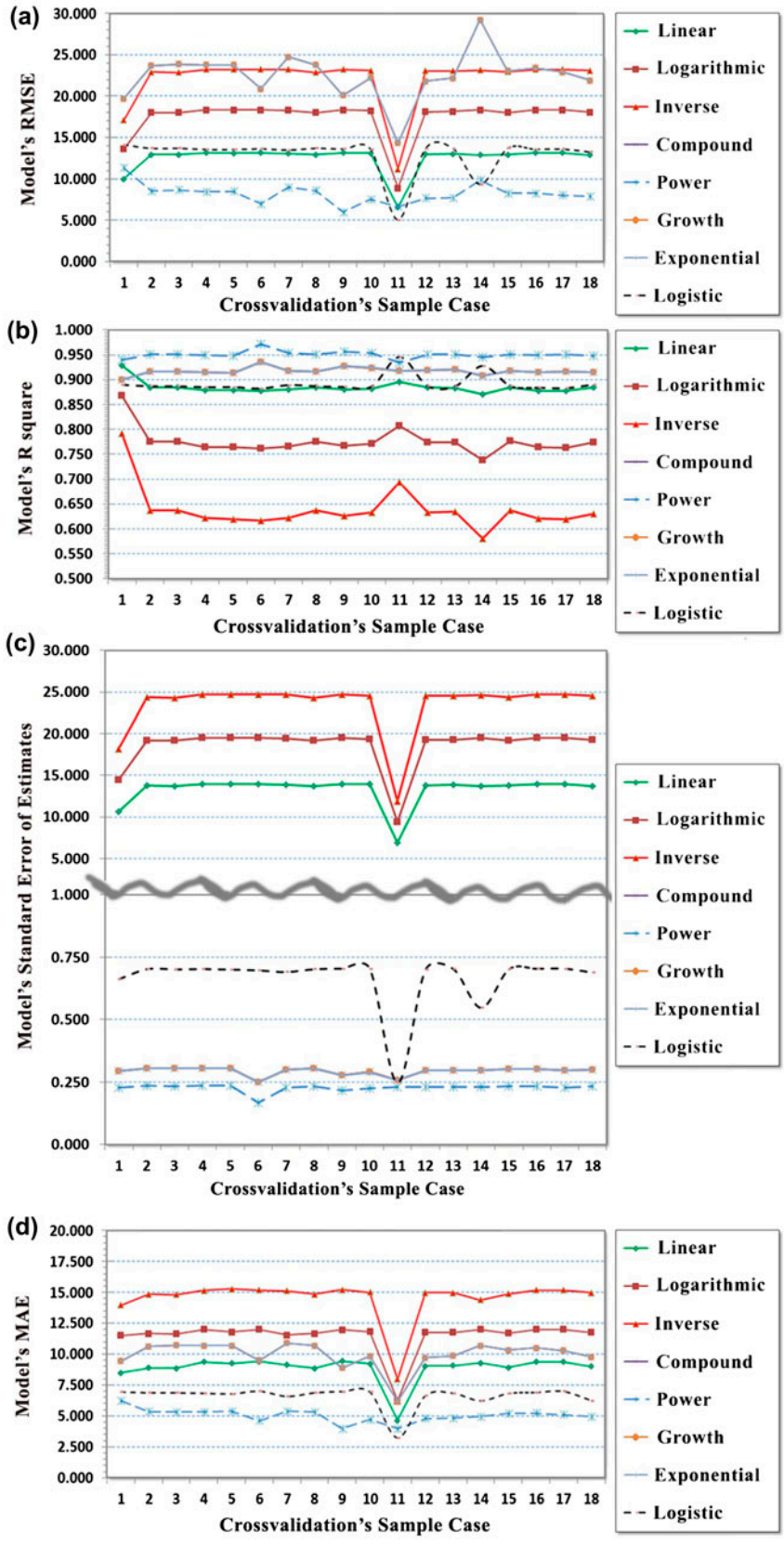

Fig. 7. Diagrams of the various model's Error Statistics Criteria results: (a) RMSE, (b) R^2, (c) Standard Error of Estimates, and (d) MAE vs. cross-validation's sample case.

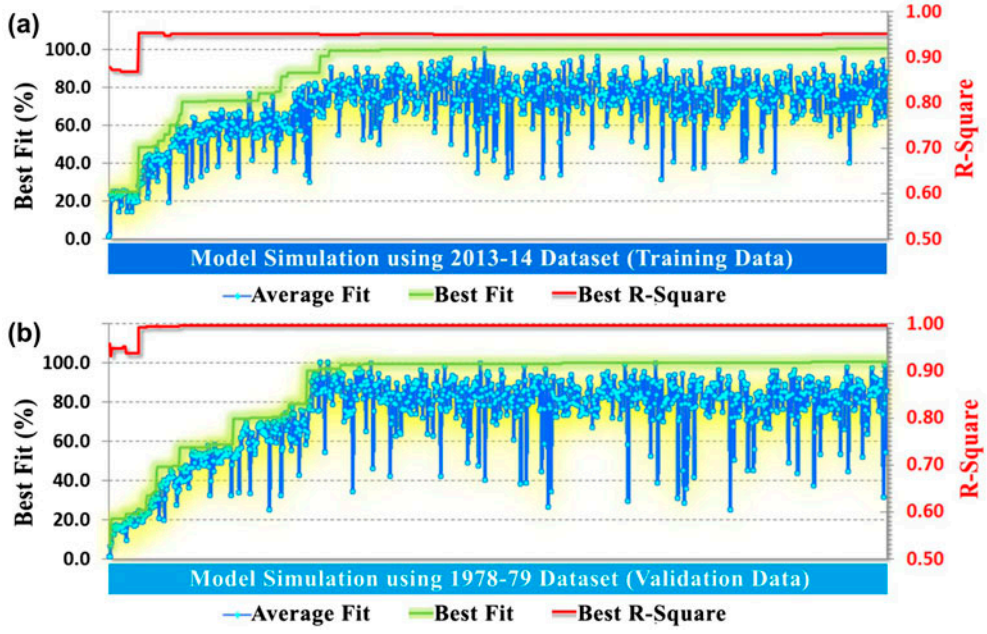

Fig. 8. Results of model simulation using: (a) 2013–14 data set (training data) and (b) 1978–79 data set (validation data).

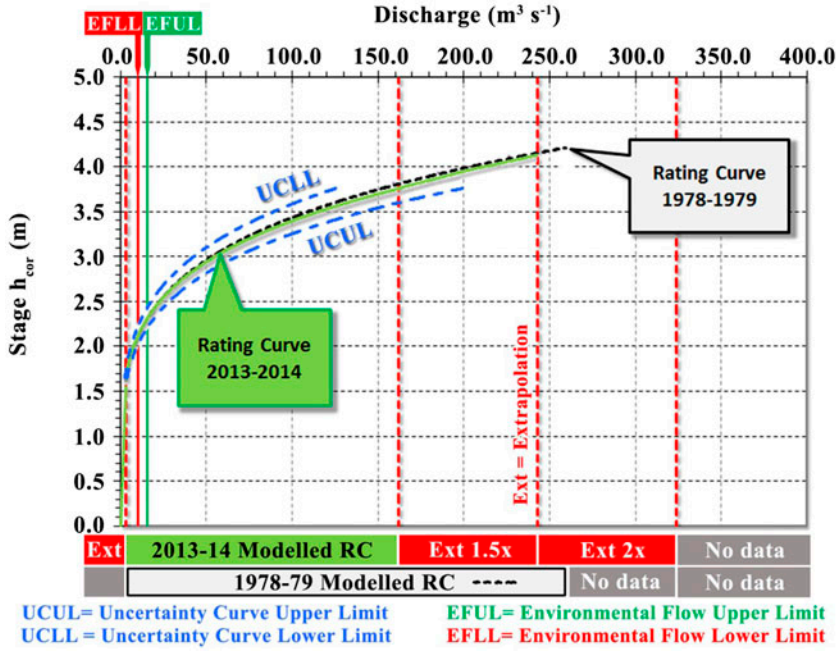

Fig. 9. The final RCs [$RC_{(1978–1979)}$ and $RC_{(2013–2014)}$] that were developed with power model, uncertainty upper and lower limits curves for years 2013–2014 data set and environmental flow upper and lower limits.

vertical reference (adjusted for 2013–2014 datum and channel cross section's geometry) and a_{0adj} is the level corresponding to zero flow rate above the same adjusted reference, while numbers 0.3115 and 4.6711 are the equation's parameters (calibration coefficients). The first is the c constant, while the second one is the regression coefficient $b1$.

The resulted power model (Eq. (6)) of 1978–1979 $h(t) - Q(t)$ data series was selected as the best model ($N = 18$, RMSE = 7.881, $R^2 = 0.9974$, Adjusted

R^2 = 0.9973, Sig. = 0.000 and MPI Index = 1.000), for 1978–1979 data. Results of the developed historic $RC_{(1978–1979)}$ showed also a low RMSE (7.881) and a high R^2 (0.9974) and even they are better than the recent curve's $RC_{(2013–2014)}$, there is a probability for a possible overfitting of 1978–1979 data, which however, can't be defined with confidence because the channel cross-section's data, geometry, datum and conditions for 1978–1979 time period were unknown, since only $h(t) - Q(t)$ data were provided from hydroscope [26]. Moreover, it was observed that the relation (Eq. (6)) between stage and discharge (for 1978–1979 data series) was modified in the period of shifting control (time period 1978–2013) into a new relation (Eq. (5)) between stage and discharge (for 2013–2014 data series). This modification is considered to be logical in a time period of 35 years. The relation between stage and discharge can be modified by a great number of factors that result in changes in the shape and position of the RC, or in loops in the RC. Principal factors that affect the RC include [19,38,41]: (a) changes to the channel cross section due mainly to scour and fill; (b) growth and decay of aquatic vegetation; (c) log or debris jams (an accumulation of logs and other organic debris which blocks the flow of a stream of water); (d) variable backwater; (e) rapidly changing discharge; (f) discharge to or from overbank areas, and (g) ice. Changes in channel geometry, such as scour or fil; and/or changes in flow conditions, such as vegetal growth, will cause shifts in the discharge rating where slope is a factor, just as they cause shifts in simple stage–discharge relations.

Moreover, the statistical t tests' [21] (with 95% confidence interval of the difference) results on validation, revealed that there is no statistically significant difference (ssd) between the discharges means of the two datasets and the esc. The results of the validation analysis between two sample datasets for model simulation and comparison, and error estimation showed that the data fitting of the selected power model was very satisfactory, and the stability of the developed relationship (Eq. (5)) is robust and also results are very close to the validation data set with the primary data with $h(t)$ and $Q(t)$ measurements in years 1978–1979 from hydroscope [26]. Finally, the results of model's validation, using the two different methods (a) cross-validation method and (b) validation method between two sample datasets [$N_{(2013–2014)}$ and $N_{(1978–1979)}$], were converge to the same output that the data fitting of the selected power model for the $RC_{(2013–2014)}$ was very satisfactory, and the stability of the developed relationship (Eq. (5)) was robust.

5. Conclusions

In Thessaly region, the agricultural sector is the main consumer of water (total annual water demand of 1.5–2.0 × 10^9 m^3), which approximately accounts for 95% of the total demands of the region [30]. The River Pinios is contributing to the agricultural sector with its discharges used mainly for irrigation purposes. However, the extreme river water withdrawals for irrigation purposes are disrupting river's good state. The Spearman's rho statistical test between the discharge $Q_{(2013–2014)}$ and 2013–2014 rainfall datasets for daily, 2-day moving average, 3-day moving average and 10-day rainfall, resulted in medium and low correlation coefficients of 0.444, 0.490, 0.502 and 0.150, respectively. This is indicating that beyond rainfall, there are other factors influencing the Pinios River discharge such as flows from: mountainous water springs, tributaries, snow melting, shallow groundwater contributions, etc. It was observed, that the summer and autumn months (June–October) of recent and also July–September of historic years presented low to zero discharges. These are below the estimated environmental flow upper (safe) limit or EFUL (16.31 m^3 s^{-1} for 2013–14 and 15.13 m^3 s^{-1} for 1978–79) and even below the environmental flow lower (critical) limit or EFLL (10.00 m^3 s^{-1} for 2013–14 and 9.28 m^3 s^{-1} for 1978–79) [30] of the Pinios River. This environmental risk state (river discharges below EFLL) is due to low summer input flows, low to zero summer rainfalls, demanding agricultural management (extreme river water withdrawals for irrigation purposes) and it must be taken care off with proper environmental and agricultural management and emergency policy measures in order to protect the riverine environment.

The results and statistical analysis of hydrological data showed that Froude number during the measurement period is oscillating from 0.109 to 0.283 (mean Fr = 0.172, standard deviation Std D = 0.0406). Therefore, in all cases Fr < 1, which means that the water flow of the River Pinios at Giannouli, Larissa station is, classified as subcritical flow. Moreover, based on the parameters measurements of the river Pinios (P145) until December 2014, on the modelling analysis and results (regression analysis, curve fit, F statistic (F test of model fit), ANOVA statistical analysis, RMSE, R^2, SEE, MAE and MAD D(%) of measured $Qm(t)$ vs. predicted values $Qr(t)$ of the RC) and also on the models' classification and on the proposed MPI, the power model was selected as the best fit model. This model was used for the compilation and best fit of the streamflow RC for this monitoring station. It was concluded that the following model (Eq. (5)) is the best approximation for curve's best fit, so far.

$$Qr = 0.3540 * (h - a_0)^{4.5502} \ (\mathrm{m^3\ s^{-1}}) \quad (7)$$

with RMSE = 8.228, R^2 = 0.9504, Adjusted R^2 = 0.9749, SEE = 0.2277, MAE = 5.060, mean MAD D(%) = 2.191 and MPI Index = 0.980.

The logarithmic extrapolation of the RC is ranging on discharges from 0.01 to 3.15 $m^3\ s^{-1}$ (low discharges) and from 162.06 to 243.09 $m^3\ s^{-1}$ (medium and high discharges), according to ISO 1100-2, (1998) [12] and Rantz et al. [41], and is particularly suited to channel control conditions for medium and high flows. Low-flow extrapolation of an RC is often required in the management of surface water resources and in their supply for domestic, industrial, agricultural or environmental uses. Unfortunately, there is no assurance that the extrapolation for low flows is precise, but the extrapolation of the present study seems to be a reasonable one. In order to acquire that assurance with statistical confidence and validate the lower extrapolation part of the RC, accurate low-flow discharge (from 0.100 to 3.148 ($m^3\ s^{-1}$)) and stage measurements are required. The upper extrapolation of the $RC_{(2013–2014)}$ at the "Ext-1.5x" part although it is underestimating the data is very close to the $RC_{(1978–1979)}$ curve. When the extrapolation goes within the "Ext-2x" part, it is also underestimating the data, and the higher in $Q(t)$ the extrapolation is, the higher the departure from the $RC_{(1978–1979)}$ curve is.

It is concluded that for the Giannouli, Larissa monitoring station the rating should not be extrapolated beyond 1.5 times the largest measured discharge because extensive errors can result if the RC is extrapolated beyond the measured range of discharges on large scales without consideration of the cross-section geometry and the effective roughness. The extrapolated upper parts of the RC should be used in cases where high flows occur in Pinios River and it is very difficult or impossible to measure the streamflow discharges during the flood events.

Model validation, model comparison and error estimation [22–25] is a crucial part of the study and it was based on two separate methods: (a) cross-validation method and (b) validation method between two sample datasets. It was observed that the developed relation (Eq. (6)) between stage and discharge (for 1978–1979 validation data) was modified in the period of shifting control (time period 1978–2013) into a new relation (Eq. (5)) between stage and discharge (for 2013–2014 recent data). This modification is considered to be logical in a time period of 35 years. The results of model's validation by using the aforementioned two methods, the error statistics criteria and the proposed MPI, were converge to the same output, that the data fitting of the selected power model for the $RC_{(2013–2014)}$ was very satisfactory and the stability of the developed new relationship (Eq. (5)) was robust.

The resulted streamflow RC and the extrapolated parts of the curve, the rainfall vs. discharge and environmental flows analysis, the river bed variations analysis and the performed hydraulic properties estimates are proposed to serve as hydrological assisting tools for environmental water resources and irrigation management in the wider local area of the Giannouli, Larissa monitoring station, of the Pinios River basin in Central Greece. These assisting tools will help water authorities accurately and quickly estimate river's water quantities and variation, with a minimum cost and effort and they could be used for irrigation management, groundwater recharge, environmental flow estimation and monitoring, flood protection and other purposes.

Finally, it should be stressed that this research is ongoing and further measurements are due, expecting that a more comprehensive data set could probably rectify–modify the calculated results thus leading to improved hydrological modelling and also better fit of the water flow RC for this station.

Acknowledgements

Data in this paper are collected in the framework of the elaboration of the national water resources monitoring network, supervised by the Special Secretariat for Water–Hellenic Ministry for the Environment and Climate Change. This project is elaborated in the framework of the operational programme "Environment and Sustainable Development" which is co-funded by the National Strategic Reference Framework (NSRF) and the Public Investment Program (PIP).

References

[1] K. Schulze, M. Hunger, P. D¨oll, Simulating river flow velocity on global scale, Adv. Geosci. 5 (2005) 133–136.
[2] V.T. Chow, Open-Channel Hydraulics, McGraw-Hill Inc., New York, NY, 1959.
[3] F.M. Henderson, Open Channel Flow, MacMillan, New York, NY, 1966.
[4] T.J. Buchanan, W.P. Somers, Discharge measurements at gauging stations, Chapter A8 in Techniques of Water-Resources Investigations of the United States Geological Survey. USGS Publications, Washington, DC, 1969.
[5] R.H. McCuen, Hydrologic Analysis and Design, second ed., Prentice Hall, Upper Saddle River, NJ, 1998.
[6] B.R. Munson, D.F. Young, T.H. Okiishi, Fundamentals of Fluid Mechanics, fourth ed., John Wiley and Sons Inc, New York, NY, 2002.

[7] A. Osman Akan, Open Channel Hydraulics, Elsevier, Oxford, UK, 2006.
[8] M.H. Chaudhry, Open-Channel Flow, second ed., Springer, New York, NY, 2008.
[9] E. Hatzigiannakis, A. Filintas, A. Ilias, G. Arampatzis, A. Panagopoulos, I. Hatzispiroglou, A first approach on compilation of a flow rating curve and riverbed variation of Pinios River at Giannouli monitoring station Larissa-Central Greece, for environmental water resources management, Proceedings of 12th International Conference on Protection and Restoration of the Environment, June 29–July 3, 2014, Skiathos Island, Greece, ISBN: 978-960-88490-6-8 (2014) 98–105.
[10] E. Hatzigiannakis, A. Filintas, A. Ilias, A. Panagopoulos, G. Arampatzis, I. Hatzispiroglou, A second approach on water flow rating curve and riverbed variation of Pinios River at Giannouli-Larissa monitoring station in Central Greece, for environmental and agricultural water resources management, Proceedings of 10th International Hydrogeological Congress of Greece, October 8–10, 2014, Thessaloniki, Greece, ISBN: 978-960-88816-6-2 (2014) 231–240.
[11] G. Corato, T. Moramarco, T. Tucciarelli, Discharge estimation combining flow routing and occasional measurements of velocity, Hydrol. Earth Syst. Sci. 15 (2011) 2979–2994.
[12] ISO 1100-2:1999, Hydrometry—Measurement of liquid flow in open channels—Part 2: Determination of the stage-discharge relationship, ISO (International Standards Organisations), International Standard, Geneva, Switzerland, ISO 1100-2, 1998.
[13] R.W. Herschy, Hydrometry: Principles and Practice, second ed., John Wiley and Sons, New York, NY, 1999.
[14] ISO 1100-2:2010, Hydrometry—Measurement of liquid flow in open channels—Part 2: Determination of the stage-discharge relationship, ISO (International Standards Organisations), International Standard, third ed., 2010-12-01, Geneva, Switzerland, ISO 1100-2, 2010.
[15] B. Abraham, J. Ledolter, Statistical Methods of Forecasting, John Wiley and Sons, New York, NY, 1983.
[16] Valeport Limited SI, Datasheet Reference: MODEL 001 or 002 version 2A, Feb 2011, Valeport, Devon, UK, 2011.
[17] BS ISO 2537:2007, Hydrometry, Rotating-element current-meters British Standards Institution, 29 June 2007, ISBN978 0 580 52904 7, BS ISO 2537, (2007).
[18] D.L. Collins, Computation of records of streamflow at control structures: US Geological Survey Water-Resources Investigations, Report, 77–8, (1977).
[19] E.J. Kennedy, Discharge ratings at gaging stations: US Geological Survey Techniques of Water-Resources Investigation Report, Book 3, Chapter A10, 1984, 59.
[20] E. Anastasiadou-Partheniou, G. Terzidis, E. Hatzigiannakis, Discharge-stage curves for Almopaio river, Proceedings of the 8th National Conference of the Hellenic Hydrotechnical Association, 19–21 April 2000, Athens, Greece, (2000), 327–334 (in Greek with english abstract).
[21] M.J. Norusis, SPSS 17.0 Guide to Data Analysis, Englewood Cliffs, Prentice Hall, USA, 2008.
[22] S. Arlot, A. Celisse, A survey of cross-validation procedures for model selection, Stat. Surv. 4 (2010) 40–79.
[23] M. Stone, Cross-validatory choice and assessment of statistical predictions, J. Roy. Stat. Soc. Ser. B 36 (1974) 111–147.
[24] S. Geisser, The predictive sample reuse method with applications, J. Am. Stat. Assoc. 70 (1975) 320–328.
[25] P.L. Bartlett, S. Boucheron, G. Lugosi, Model selection and error estimation, Mach. Learn. 48 (2002) 85–113.
[26] Hydroscope, Stage and Discharge data-Giannouli Station-Year 1978–1979, Hydroscope Project, 2010. Available from: <http://hydroscope.gr/>.
[27] A. Filintas, Land use systems with emphasis on agricultural machinery, irrigation and nitrates pollution, with the use of satellite remote sensing, geographic information systems and models, in watershed level in Central Greece, MSc thesis, Department of Environment, University of Aegean, Mitilini, Greece, 2005.
[28] G. Migiros, G. Bathrellos, H. Skilodimou, T. Karamousalis, Pinios (Peneus) river (Central Greece): Hydrological—Geomorphological elements and changes during the Quaternary, Cent. Eur. J. Geosci. 3 (2) (2011) 215–228.
[29] D. Mountrakis, E. Sapountzis, A. Kilias, G. Eleftheriadis, G. Christofides, Paleogeographic conditions in the western Pelagonian margin in Greece during the initial rifting of the continental area, Can. J. Earth Sci. 20 (1983) 1673–1681.
[30] A. Filintas, Environmental study of pollution and quality of water resources, hydrogeology and hydrochemistry of the Pinios riverine hydrosystem of Thessaly, by the use of field research, laboratory analysis, Data Bases, GPS, GIS, Remote Sensing and statistical analysis, Project Free-Med: Fleuves et Rivieres Edpaces D'Equilibre pour la Mediterranee (Rivers Spaces of Balance for the Mediterranean), EVS, Region of Thessaly, Larissa, Greece, 2011, (with extended abstracts in Greek and French).
[31] V. Jacobshagen, Geologie von Griechenland. (Geology of Greece), Gebr. Borntraeger, Berlin–Stuttgart, 1986.
[32] G. Katsikatsos, G. Migiros, M. Triantaphyllis, A. Mettos, Geological structure of Internal Hellenides (E. Thessaly-SW Macedonia-Euboea-AtticaNorthern Cyclades Islands and Lesvos), The Instituto Geológico y Minero de España, Geology & Geophisics Research, Special Issue, (1986) 191–212.
[33] A. Ilias, E. Hatzigiannakis, A. Panoras, Protocol of streamflow velocity and discharge measurements in Rivers, Land Reclamation Institute of Thessaloniki, Hellenic Agricultural Organization "Demeter", Sindos-Thessaloniki, Greece, 2013.
[34] ISO 748:2007, Hydrometry—Measurements of liquid flow in open channels using current-meters or floats, International Standard, fourth ed., 15 October 2007, ISO International Standards Organisations, Geneva, Switzerland, ISO 748, 2007.
[35] N.R. Draper, H. Smith, Applied Regression Analysis, second ed., John Wiley and Sons, New York, NY, 1981.
[36] A. Filintas, Land use evaluation and environmental management of biowastes, for irrigation with processed wastewaters and application of bio-sludge with agricultural machinery, for improvement-fertilization of soils and cultures, with the use of GIS-Remote Sensing, Precision Agriculture and Multicriteria Analysis., PhD Thessis, PGP Theofrasteio: Environmental and Ecological Engineering, Dept. of Environment, University of the Aegean, Mitilini, Greece, 2011.

[37] G. Stamatis, K. Parpodis, A. Filintas, E. Zagana, Groundwater quality, nitrate pollution and irrigation environmental management in the Neogene sediments of an agricultural region in central Thessaly (Greece), Environ. Earth Sci. 64 (2011) 1081–1105.
[38] R.W. Herschy, Streamflow Measurement, second ed., Chapman & Hall, 1995.
[39] J.D. Fenton, R.J. Keller, The Calculation of Streamflow fromMeasurements of Stage, Water, Technical Report 01/6, Cooperative Research Centre for Catchment Hydrology, Melbourne, Australia, 2001.
[40] R.W. Herschy, The uncertainty in a current meter measurement, Flow Meas. Instrum. 13 (2002) 281–284.
[41] S.E. Rantz, et al., Measurement and computation of streamflow, Volume 2 Computation of Discharge, US Geological Survey Water Supply Paper 2175, 1982.
[42] I.K. Kalavrouziotis, A.T. Filintas, P.H. Koukoulakis, J.N. Hatzopoulos, Application of multicriteria analysis in the management and planning of treated municipal wastewater and sludge reuse in agriculture and land development: The case of Sparti's wastewater treatment plant, Greece, Fresenious Environ. Bull. 20(2) (2011) 287–295.
[43] A. Filintas, Evaluation Methodology of the environmental pilot projects of the program Free-MED, Fleuves et Rivieres Edpaces D'Equilibre pour la Mediterranee (Rivers Spaces of Balance for the Mediterranean) using multicriteria decision analysis models, data bases and statistical analysis, Region of Thessaly, Larissa, Greece, 2011.
[44] A. Filintas, Evaluation study of environmental pilot projects of Thessaly Region in Greece, for the international program Free-MED—"Rivers spaces of balance for the Mediterranean", with use of multicriteria models, data bases and statistical analysis, Proceedings of ARSA 2012 V, International Conference on Advanced Research in Scientific Fields, 3–7 December, Slovakia, paper ID-1527, (2012), 1323–1328.
[45] D.L. Stufflebeam, Evaluation models. New Directions for, Evaluation 2001(89) (2001) 7–98.
[46] J.W. Creswell, V.L.P. Clark, Designing and conducting mixed methods research, Sage, Thousand Oaks, CA, 2006.
[47] A. Filintas, P. Dioudis, G. Stamatis, J. Hatzopoulos, T. Karyotis, Environmental assessment of groundwater nitrate pollution from agricultural wastes and fertilizers in Central Greece watersheds using remote sensing and GIS, Proceedings of 3rd International Conference AQUA 2008 on: Water Science and Technology with emphasis on water & climate, 16–19 October, Athens, Greece, ID-02, (2008) 1–10.
[48] V.B. Sauer, Standards for the Analysis and Processing of Surface-Water Data and Information Using Electronic Methods, U.S. Geological Survey Water-Resources Investigations Report 01–4044, 91, 2002.
[49] E. Hatzigiannakis, E. Anastasiadou-Partheniou, Finite Differences Model for Simulation of Flood Wave Propagation in a Pinios River Section, Selected Papers of Int. Conf. of Computational Sciences and Engineering, Hania, Crete island, Greece,7A, (2006) 701–704.
[50] E. Koutseris, A. Filintas, P. Dioudis, Environmental control of torrents environment: One valorisation for prevention of water flood disasters, WIT Transactions on Ecology and the Environment, WIT Press 104 (2007) 249–259.
[51] E. Koutseris, A. Filintas, P. Dioudis, Antiflooding prevention, protection, strategic environmental planning of aquatic resources and water purification: The case of Thessalian basin, in Greece, Desalination 250 (1) (2010) 318–322.
[52] S.C. Larson, The shrinkage of the coefficient of multiple correlation, J. Educ. Psychol. 22 (1931) 45–55.
[53] F. Mosteller, J.W. Tukey, Data analysis, including statistics, in: G. Lindzey, E. Aronson, (Eds.), Handbook of Social Psychology, 2, Addison-Wesley, 1968.
[54] M. Rudemo, Empirical choice of histograms and kernel density estimators, Scand. J. Stat. 9 (1982) 65–78.
[55] C. Stone, An asymptotically optimal window selection rule for kernel density estimates, Ann. Stat. 12(4) (1984) 1285–1297.
[56] L. Devroye, T.J. Wagner, Distribution-free performance bounds for potential function rules, IEEE Trans. Inf. Theory25(5) (1979) 601–604.
[57] L. Breiman, P. Spector, Submodel selection and evaluation in regression. The X-random case, Int. Stat. Rev. 60(3) (1992) 291–319.